FRACTURE AND FATIGUE EVALUATION OF DAMAGE TOLERANT Al-Li ALLOYS FOR AEROSPACE APPLICATIONS

R.J.H. Wanhill, L. Schra and W.G.J. 't Hart*

Qualification of Al-Li alloys for damage tolerant aerospace structures requires extensive testing and evaluation. In this paper the emphasis is on fracture and fatigue crack growth properties of two candidate sheet alloys, 2091 and 8090, compared with the conventional and widely used 2024 alloy. The relative merits of these materials are assessed, problem areas are indicated, and a survey is made of the type of qualification programme necessary for damage tolerant Al-Li aerospace structures.

INTRODUCTION

Modern Al-Li alloy development is motivated by prospective weight savings owing to decreased density and increased stiffness as compared with conventional alloys. Improvements in density and stiffness are joint consequences of lithium additions. Thus alloy development may be considered successful – from an engineering viewpoint – if other properties are simply maintained. This is the development strategy for damage tolerant Al-Li alloys.

The present work concentrates on the fracture and fatigue crack growth properties of two candidate damage tolerant Al-Li sheet alloys, 2091 and 8090, compared with the conventional and widely used 2024 alloy. Based on the results the current status of damage tolerant Al-Li sheet alloys is assessed and problem areas are indicated. Finally, a survey is made of the type of testing and evaluation programme necessary for qualifying damage tolerant Al-Li alloys for aerospace structures.

* National Aerospace Laboratory NLR, Amsterdam, The Netherlands.

EXPERIMENTAL

The materials and test programme are surveyed in table 1. Full experimental details are given in reference (1). The 2091 alloy was in three heat treatment conditions, TX, TY and T8X, representing successive attempts to achieve strength-fracture toughness combinations equivalent to those of 2024-T3.

Strength, Fracture Toughness and Crack Resistance

Comparisons of strength, fracture toughness and crack resistance (K_R curves) are given in figures 1-3. The K_c values and crack resistances of 2091-T8X and 8090-T81 were similar to those of 2024-T3, albeit at yield strengths 20-50 MPa lower. The fracture properties of 2091-TX and 2091-TY were unacceptable: little or no stable crack growth occurred except in T-L specimens of 2091-TY. The large effect of successive ageing treatments on the fracture properties of 2091 will be discussed later in this paper.

TABLE 1 - Materials and Test Programme.

Supplier	Material	Ageing Treatment	Sheet Thickness (mm)
CEGEDUR PECHINEY	2091-TX 2091-TY 2091-T8X	48 hr at 150 °C 12 hr at 150 °C 12 hr at 135 °C	1.6 1.7
ALCAN	8090-T81	12 hr at 150 °C	1.6
ALCOA	2024-T3	Naturally aged	1.6

- Mechanical properties according to ASTM Standard E8-83
- Fracture toughness and R-curves for 500 mm wide centre cracked tension (CCT) panels according to ASTM Standard E561-81
- Fatigue crack growth in 110 mm wide centre cracked tension (CCT) specimens
  - constant amplitude loading, R = 0.1
  - gust spectrum loading MINITWIST, clipping level III
  - constant amplitude loading, R = 0.5, and underloads + peak loads

Fatigue Crack Growth

Only 2091-T8X, 8090-T81 and 2024-T3 were tested for fatigue crack growth properties, owing to the poor fracture properties of 2091-TX and 2091-TY.

Crack growth lives. Figure 4 surveys the fatigue crack growth lives. Under constant amplitude loading, with or without occasional peak loads, 8090-T81 was better than 2091-T8X and 2024 -T3 . However, under MINITWIST loading 2024-T3 was much superior.

Constant amplitude crack growth rates. Figure 5 compares the data for R = 0.1. At lower ΔK 8090-T81 had the lowest rates, but at higher ΔK 2091-T8X was superior. Crack growth rates in 2024-T3 were more or less intermediate between those of the Al-Li alloys. Similar trends were found for R = 0.5 (1).

Gust spectrum (MINITWIST) crack growth rates. Figure 6 compares the data for clipping level III, which is a reasonable reduction of peak loads for macrocrack growth studies (2). 2024-T3 was superior over virtually the entire range of crack lengths. The shapes of the crack growth rate curves indicate that the peak loads in severe flights had large and persistent retarding effects on crack growth (2). In other words, more crack growth retardation occurred in 2024-T3.

Crack growth behaviour due to occasional peak loads. Figure 7 shows results of the constant amplitude and underload + peak load tests. The effects of peak loads, i.e. crack growth delays, are more consistent with the alloy rankings for constant amplitude loading than for MINITWIST loading: longer delays tend to correlate with lower constant amplitude crack growth rates. This is not surprising, although an additional factor is that longer delays should also be associated with lower yield strength (2091 -T8X and 8090-T81 had longitudinal yield strengths 40-50 MPa lower than that of 2024-T3) because lower strengths result in larger peak load plastic zones.

DISCUSSION

Material-Property Rankings

Table 2 surveys the relative performances of the three damage tolerant materials. The mechanical properties, fracture toughnesses and crack resistances of 2091-T8X and 8090-T81 were inferior – though sometimes only slightly – to those of 2024-T3, but the rankings for fatigue crack growth varied.

Fracture Toughness and Crack Resistance

Stable and unstable crack growth in 2091-T8X, 8090-T81 and 2024-T3 occurred in the slant mode typical of ductile, plane stress fracture. The fractographic characteristics were also ductile (microvoid coalescence and shear walls) except that unstable crack growth in 2091-T8X was 50 % intergranular (3).

TABLE 2 - Material-Property Rankings: ● 2091-T8X, o 8090-T81, ▲ 2024-T3.

Property		Higher Ranking →		
Yield and ultimate tensile strengths		●	o	▲
Tensile elongation		o	●	▲
Fracture toughness K_c and crack resistance		o	●	▲
Fatigue crack growth	constant amplitude, R=0.1 and R=0.5	▲ /	●	o
	gust spectrum MINITWIST	●	o	▲
	constant amplitude and underloads + peak loads	●	▲	o

The 2091-TX and 2091-TY alloys failed anomalously. Stable crack growth (if any) was slant with extensive plasticity, but unstable crack growth was macroscopically flat and brittle. This change was accompanied by low fracture toughness, low crack resistance and a transition from ductile transgranular fracture (microvoid coalescence and shear walls) to 100 % intergranular fracture (3). Also, crack jumping followed by temporary crack arrest was characterized by intergranular fracture changing to ductile fracture (1). Figure 8 shows the relations between these effects and the load-COD records.

Additional evidence that the failure modes for 2091-TX and 2091-TY were anomalous is provided by the Hahn and Rosenfield fracture criterion (4) which predicts – in a slightly modified form – that the transition to full plane stress (slant mode) fracture occurs when

$$2r_y = \frac{1}{\pi} (K_c/\sigma_y)^2 > 3t \qquad (1)$$

where $2r_y$ is the Irwin plane stress plastic zone size and t is the sheet thickness. Figure 9 compares the instability failure modes with the Hahn and Rosenfield criterion and shows that three of the four flat failure modes in 2091-TX and 2091-TY should have been slant.

The foregoing observations suggest that 2091-TX and 2091-TY were sensitive to dynamic effects, such that higher strain rates ahead of crack tips resulted in increased yield stress, a change from fully ductile to intergranular fracture, and inferior crack resistance. This implies that a material like 2091-T8X, which showed a change from fully ductile stable crack growth to 50 % intergranular unstable crack growth, could have a dynamic fracture toughness K_d much lower than the quasi-static fracture toughness K_c. Thus although 2091-T8X had acceptable K_c values and

resistances to slow, stable crack growth (figures 1-3) the fail-safe crack arrest properties could be much inferior to those of 8090-T81 and 2024-T3.

Fatigue Crack Growth

The most significant result is the different rankings of the three damage tolerant alloys, table 2. A detailed fractographic examination and measurements of fracture surface roughness (1) gave the results summarised in table 3 and figure 10. Examples of the fracture topographies are shown in figure 11. (Note: K_{mf} is the mean stress intensity in flight simulation fatigue.)

TABLE 3 - Fatigue Fracture Characteristics

Material	Constant Amplitude and Constant Amplitude with Occasional Peak Loads	Gust Spectrum MINITWIST
2091-T8X	Continuum mode with isolated facets at lower ΔK; more facets at higher ΔK	Continuum mode
8090-T81	Highly faceted: faceting temporarily reduced after peak loads	Continuum mode
2024-T3	Continuum mode	Continuum mode

The fractographic examination and roughness measurements revealed obvious differences in topography and roughness, depending on material and load history. Under constant amplitude loading, with or without occasional peak loads, the fracture surface roughness of 8090-T81 was significantly greater than that of 2091-T8X and 2024-T3. But under MINITWIST loading the roughnesses were similar, cf. figures 10 and 11. Thus the superiority of 8090-T81 under constant amplitude loading (at lower ΔK, figure 5) and constant amplitude loading with occasional peak loads is due to greater roughness. In turn, this is due to inhomogeneous plastic deformation resulting in faceted fracture, crack deflection and branching, irregular crack fronts, and roughness-induced crack closure: all of which lower the crack driving force and hence the crack growth rates (1). This observation is not new. Others have reported similar correlations between fracture surface roughness and fatigue crack growth rates (5-9).

It is now necessary to explain why MINITWIST resulted in fracture surface roughnesses that were similar and generally less than those caused by constant amplitude loading. The constant amplitude and underload + peak load tests provide the most likely answer. Single peak loads resulted temporarily in flatter, less faceted crack growth in 8090-T81. The same phenomenon could occur continuously during MINITWIST loading owing to peak load

interactions, which were also responsible for the U-shaped crack growth rate curves in figure 6.

The effect of peak loads and peak load interactions is probably the activation of more slip planes in the monotonic plastic zone ahead of the crack tip, leading to more homogeneous cyclic plastic deformation and less rough fatigue fractures. This effect is likely to be a general one for damage tolerant alloys, since the overall crack growth rates are sufficiently low to ensure peak load interactions under gust spectrum loading.

The foregoing rationale does not, however, explain the inferiority of 8090-T81 with respect to 2024-T3 under MINITWIST loading, figures 4 and 6: nor the crossover of the 2091-T8X and 2024-T3 constant amplitude crack growth rate curves in figure 5. In the first case, other factors besides fracture surface roughness must be involved, for example microstructural and environmental effects on crack driving force and crack growth resistance (1). For the second case we can be more specific. The change in ranking of 2091-T8X and 2024-T3 with increasing ΔK correlates with increased faceted crack growth in 2091-T8X (1, 10). However, this did not result in significant differences in fracture surface roughness at higher ΔK, figure 10. The most likely explanation is that roughness measurements are not always discriminatory enough to detect significant changes in crack growth. For 2091-T8X these changes were: increased inhomogeneous plastic deformation (faceting) with increasing ΔK; concomitant increases in crack deflection and branching; and a decrease in crack driving force and crack growth rates relative to 2024-T3.

QUALIFICATION OF DAMAGE TOLERANT Al-Li ALLOYS

The present results and others (3, 9-13) have shown that the damage tolerant Al-Li sheet alloys 2091 and 8090 possess acceptable fracture toughness, crack resistance, constant amplitude fatigue crack growth properties (with and without occasional peak loads) and corrosion and stress corrosion resistance, as compared to conventional alloys like 2024-T3. However, there are several problem areas:

(1) At yield strengths > 325 MPa the Al-Li sheet alloys become increasingly less fracture resistant than conventional 2000 series alloys (14).

(2) Texture effects on properties should be minimised by recrystallization, which is not easy to achieve in gauges beyond 2 mm.

(3) Al-Li sheet in nominally damage tolerant tempers may be sensitive to dynamic effects on crack resistance. This means that fail-safe crack arrest properties must be investigated, using stiffened panels typical of aerospace structures.

(4) Under gust spectrum loading the long fatigue crack growth behaviour of the Al-Li sheet alloys is significantly

inferior to that of 2024-T3. This means that Al-Li applications could be restricted to fuselage structural areas whose load histories resemble constant amplitude loading with or without occasional peak loads.

(5) Besides the typical damage tolerance properties, fatigue durability is essential. In fact, durability is probably the most critical test of the ability of damage tolerant Al-Li alloys to replace conventional materials. Durability means in practice the late occurrence of widespread cracking at fastener holes in aerospace structures. In this respect the short fatigue crack growth properties are of primary importance (15).
The available information on short fatigue crack growth in Al-Li and conventional alloys indicates that growth rates under constant amplitude (16) and gust spectrum (17) loadings are comparable. But more definitive data are needed for comparing damage tolerant Al-Li and conventional sheet alloys.

Taking an overall view, it is clear that there is no simple answer to the question whether – from an engineering viewpoint – Al-Li alloys can replace conventional alloys in damage tolerant aerospace structures. Additional testing and evaluation are necessary, as also are drastic reductions in the basic materials costs. A survey of the type of testing and evaluation programme that is needed is given in table 4. The scope of such programmes requires international cooperation between alloy producers, aircraft manufacturers and research institutes. In Europe there are several programmes, of which the most extensive is that proposed by GARTEUR (Group for Aeronautical Research and Technology in EURope). This includes the industrial participants Alcan, Pechiney, British Aerospace, Dassault, Dornier, Fokker and MBB, and the national research institutes DLR, NLR, ONERA and RAE.

TABLE 4 - Al-Li Damage Tolerance Qualification Programme.

Properties	Property details	Special considerations
• Mechanical	Tensile (multi-angle, compression, bearing	Texture, temperature (225-440 K)
• Fracture toughness and crack resistance	K_c, R-curves, stiffened panel crack arrest	Texture, dynamic effects
• Fatigue life	Plain and notched specimens, structural joints; constant amplitude and flight simulation loading	Environmental effects, corrosion protection systems for structural joints
• Fatigue crack growth	Long and short cracks; constant amplitude and flight simulation loadings	Texture, environmental effects; crack growth prediction
• Corrosion	Corrosion and stress corrosion; accelerated and natural environments	Microbiological corrosion in integral fuel tanks
• Fabrication	Forming, chemical milling, adhesive bonding	Superplasticity

CONCLUDING REMARKS

In this paper the fracture and fatigue crack growth properties of two candidate damage tolerant Al-Li sheet alloys, 2091 and 8090, were compared with those of the conventional and widely used 2024 alloy. Based on the results the current status of damage tolerant Al-Li sheet alloys was assessed and problem areas indicated. Finally a survey was made of the type of testing and evaluation programme needed for qualifying damage tolerant Al-Li alloys for aerospace structures.

ACKNOWLEDGEMENT

This research was sponsored by the Netherlands Agency for Aerospace Programs (NIVR).

REFERENCES

(1) Wanhill, R.J.H. and Schra, L., NLR CR 89349, October 1989.
(2) Wanhill, R.J.H., Fat. Eng. Mater. Struct., Vol. 1, 1979, pp. 5-19.
(3) 't Hart, W.G.J., Schra, L., McDarmaid, D.S. and Peters, M., New Light Alloys, AGARD CP No. 444, 1989, pp. 5-1 - 5.17.
(4) Hahn, G.T. and Rosenfield, A.R., Applications Related Phenomena in Titanium Alloys, ASTM STP 432, 1968, pp. 5-32.
(5) Suresh, S., Met. Trans. A, Vol. 16A, 1985, pp. 249-259.
(6) Suresh, S. and Ritchie, R.O., Met. Trans. A., Vol. 13A, 1982, pp. 1627-1631.
(7) Venkatsewara Rao, K.T. and Ritchie, R.O., Acta Met., Vol. 36, 1988, pp. 2849-2862.
(8) Vasudevan, A.K., Bretz, P.E. and Miller, A.C., Mater. Sci. Eng., Vol. 64, 1984, pp. 113-122.
(9) Peters, M., Bachmann, V. and Welpmann, K., 4th International Aluminium Lithium Conference, Les Editions de Physique, 1987, pp. C3-785 – C3-791.
(10) Ohrloff, N., Gysler, A. and Lütjering, G., Ibid., pp. C3-801 – C3-807.
(11) 't Hart, W.G.J., Schra, L. and Wanhill, R.J.H., 16th Congress of the International Council of the Aeronautical Sciences, AIAA, Vol. I, 1988, pp. 75-83.
(12) Smith, C.J.E., Gray, J.A., Schra, L., Boogers, J.A.M., Braun, R., Buhl, H. and Vaessen, G., Ref, (3), pp. 7-1–7-20.
(13) Le Roy, G., Mace, R., Marchive, D., Meyer, P., Nossent, R. and Schlecht, F., Ref. (9) pp. C3-33 – C3-39.
(14) Peel, C.J., Ref. (3), pp. 21-1 – 21-9.
(15) Wanhill, R.J.H., The Behaviour of Short Fatigue Cracks, Mechanical Engineering Publications Ltd., 1986, pp. 27-36.
(16) Venkateswara Rao, K.T., Yu, W. and Ritchie, R.O., Eng. Fract. Mech., Vol. 31, 1988, pp. 623-635.
(17) Blom, A.F., AGARD Report, In Preparation.

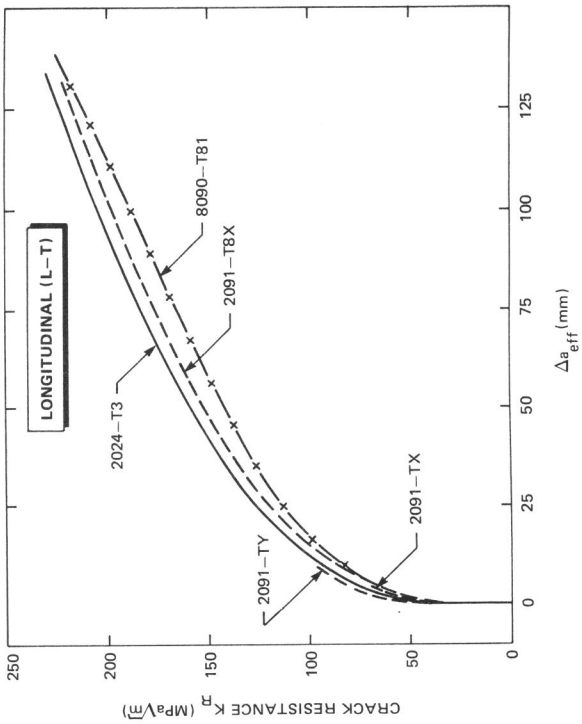

Fig. 2 Comparison of mean K_R curves for longitudinal 500 mm wide CCT panels

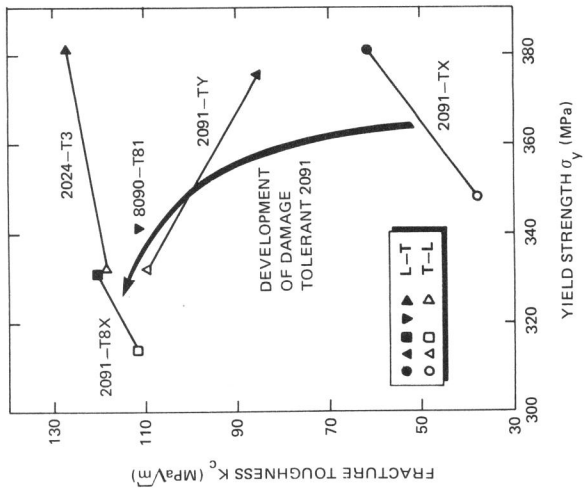

Fig. 1 Comparisons of average yield strength-fracture toughness combinations

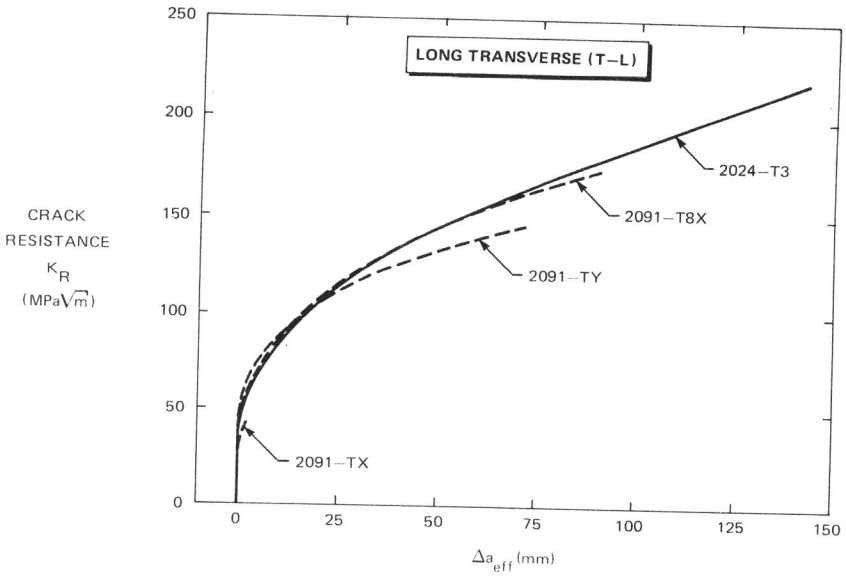

Fig. 3 Comparison of mean K_R curves for transverse 500 mm wide CCT panels

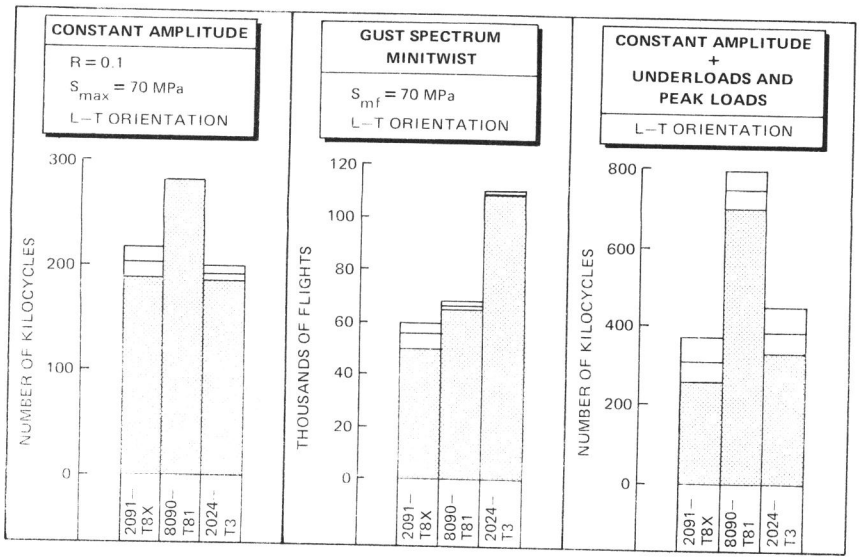

Fig. 4 Survey of fatigue crack growth lives from a = 4 mm to failure

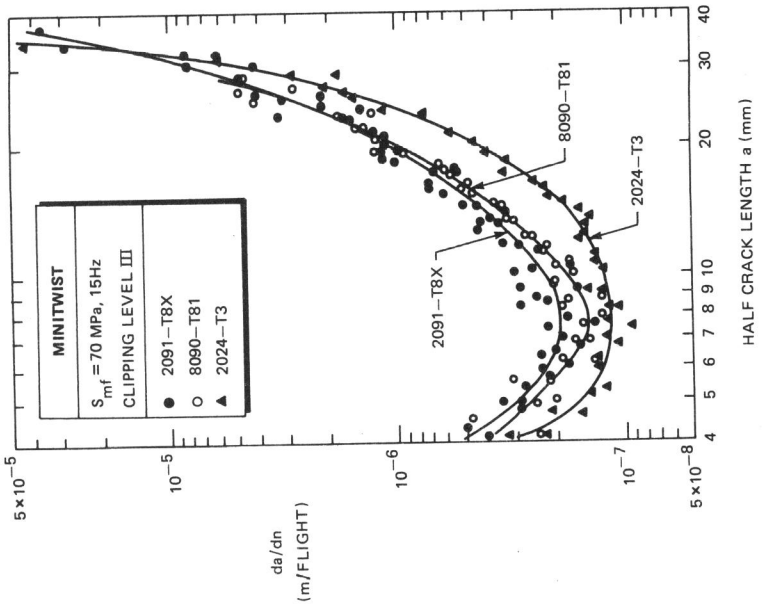

Fig. 6 Comparison of flight simulation (gust spectrum) fatigue crack growth rates

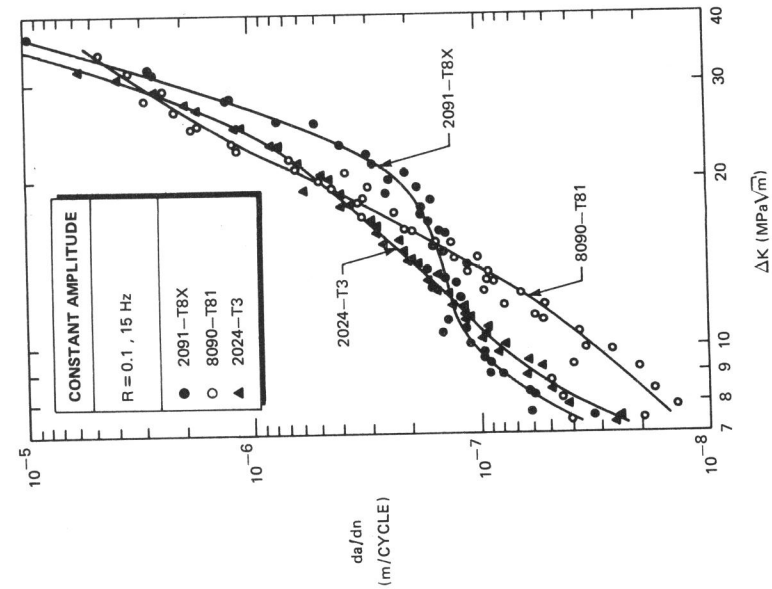

Fig. 5 Comparison of constant amplitude fatigue crack growth rates, R = 0.1

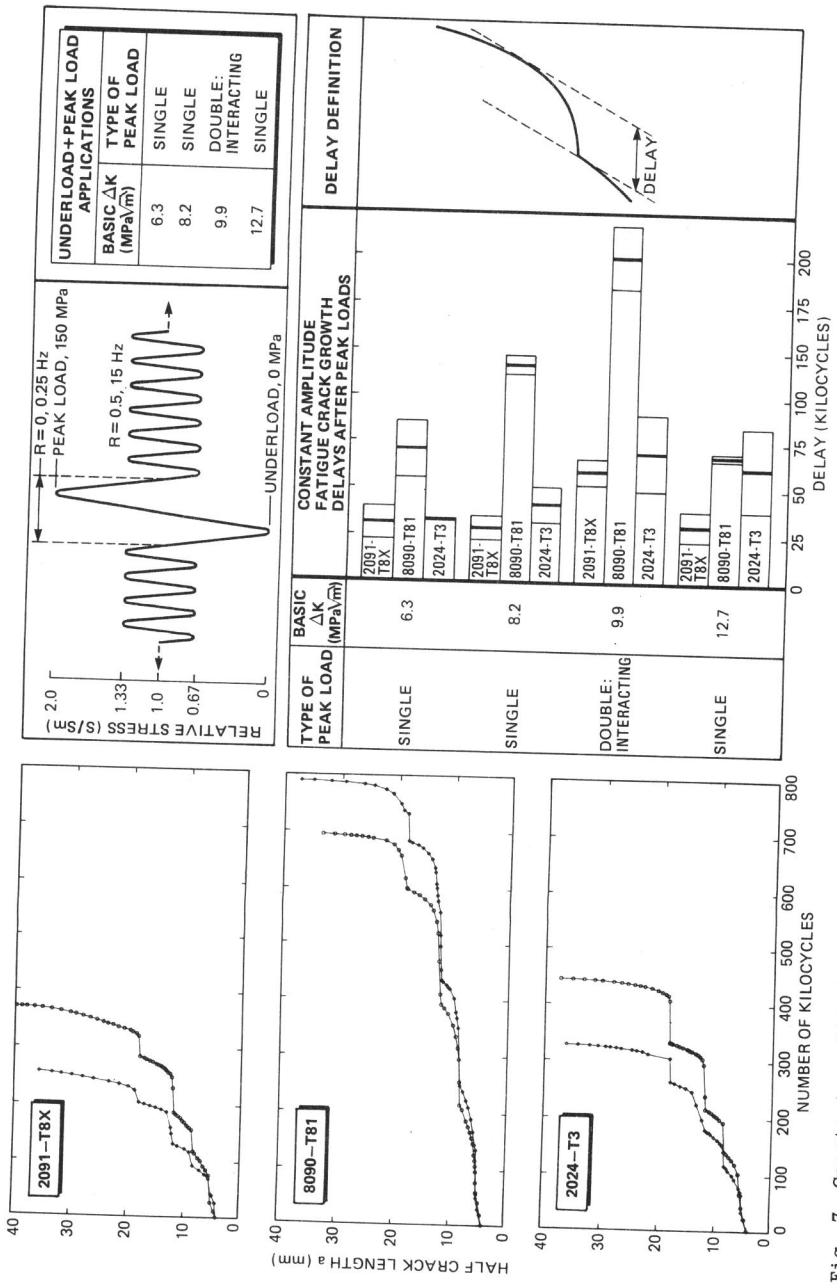

Fig. 7 Constant amplitude and occasional underload + peak load test results

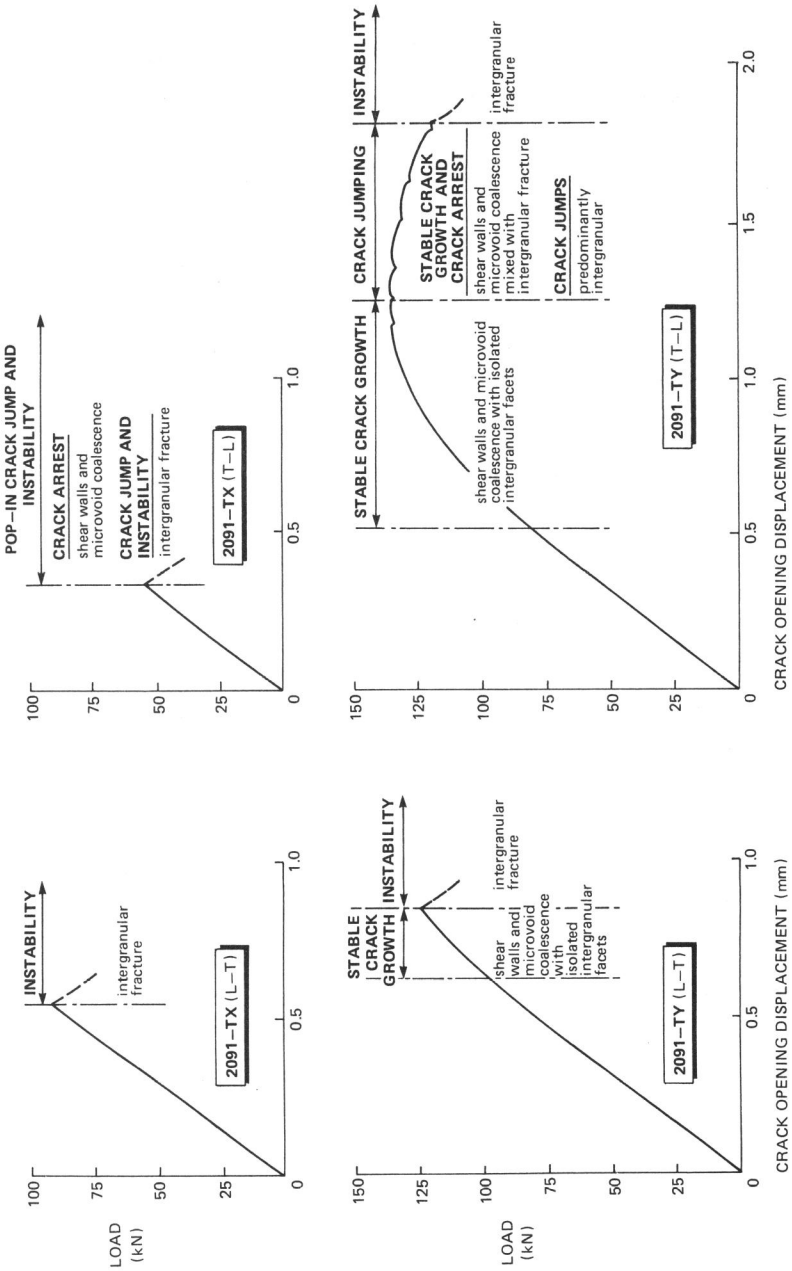

Fig. 8 Load-COD records and fracture characteristics of monotonic crack growth in 2091-TX and 2091-TY

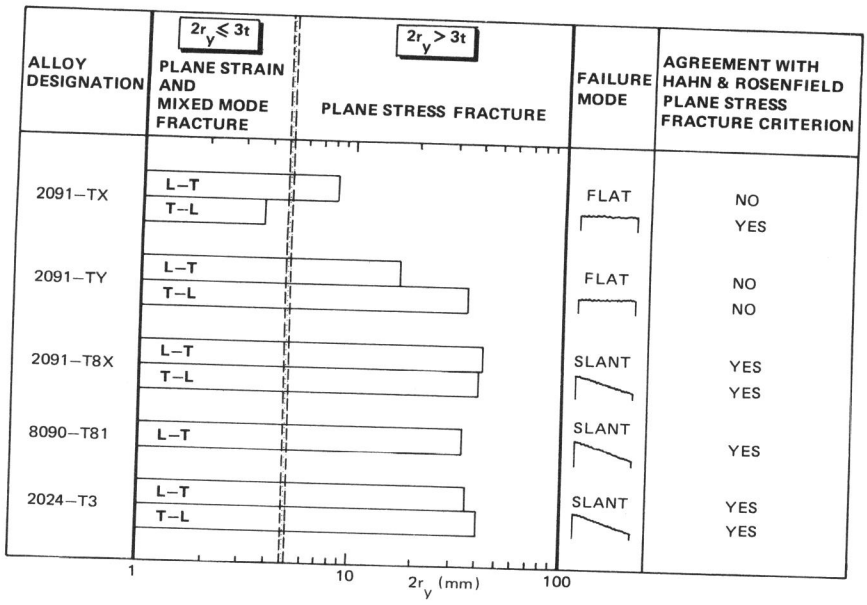

Fig. 9 Instability failure modes compared with the Hahn and Rosenfield plane stress fracture criterion

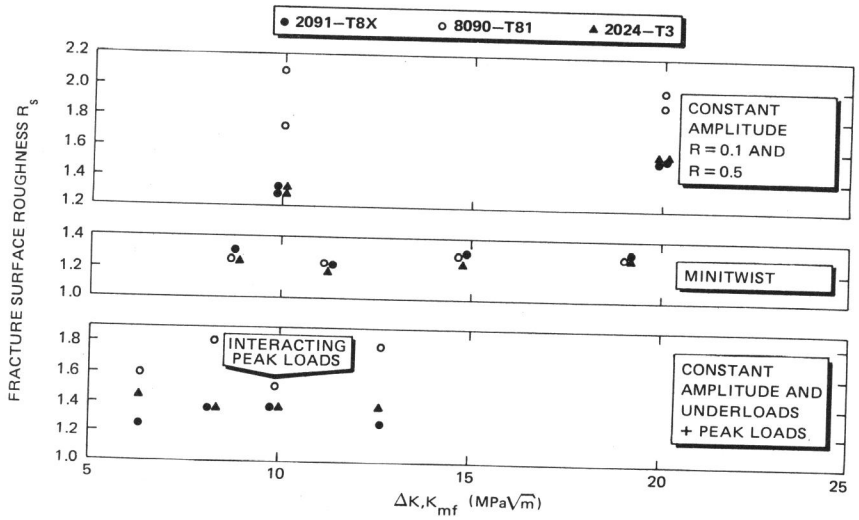

Fig. 10 Fatigue fracture surface roughnesses: each data point is the mean of six measurements

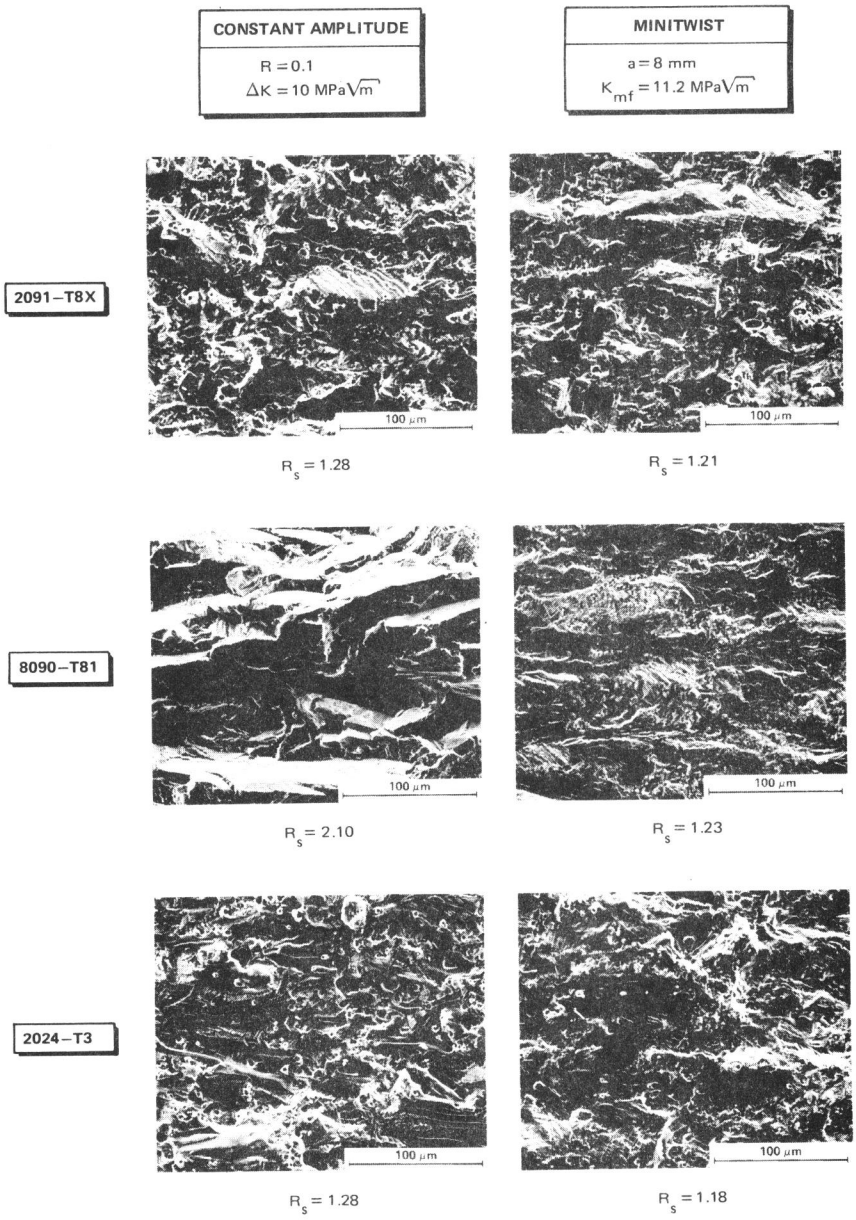

Fig. 11 Examples of fatigue fracture topographies